Synchrotron X-ray diffraction study of ZnTe at high pressure

A. Onodera[a,*], A. Ohtani[a,1], S. Tsuduki[a], O. Shimomura[b,2]

[a] *Graduate School of Engineering Science, Osaka University, Toyonaka, Osaka 560-8531, Japan*
[b] *SPring-8, Japan Atomic Energy Research Institute, Sayo, Hyogo 679-5148, Japan*

Abstract

ZnTe has been studied at high pressure to 76 GPa and at room temperature in a diamond-anvil cell using angle-dispersive X-ray diffraction technique with synchrotron radiation and an imaging plate detector. The equation-of-state parameters of the two high-pressure phases of ZnTe were for the first time derived to be $B_0 = 91.3(7.0)$ GPa and $B_0' = 0.8(1.0)$ for the cinnabar-type phase and $B_0 = 134(5)$ GPa and $B_0' = 2.4(1)$ for the *Cmcm*-type phase, respectively.
© 2007 Elsevier Ltd. All rights reserved.

1. Introduction

Most of the semiconducting II–VI and III–V compounds become metallic at high pressure as exemplified by the chalcogenides of zinc [1]. The electrical behavior of ZnTe is peculiar in that an intermediate semiconducting state appears prior to the pressure-induced metallization [1–5]. We suggested earlier, from electrical resistance and X-ray diffraction measurements simultaneously undertaken at high pressure, that the semiconductor-to-semiconductor and the semiconductor-to-metal transitions of ZnTe are both accompanied by structural phase transitions [3]. Indeed, recent X-ray diffraction studies using synchrotron radiation have determined the structures of the intermediate semiconducting phase to be the hexagonal cinnabar-type [6–11] and the metallic phase to be the orthorhombic *Cmcm*-type [9–11], respectively. Despite the growing interest in the physical properties of ZnTe at high

pressure from both experimental and theoretical viewpoints, the equation-of-state data of the two high-pressure phases have been unavailable.

The present study was undertaken to investigate the equations of state of ZnTe by X-ray diffraction measurements employing synchrotron radiation in combination with an imaging plate detector. High pressure was generated in a diamond-anvil cell either with a pressure-transmitting medium (to 76 GPa) or without the medium (to 43 GPa). The difference in the modes of pressurization was to know the effect of pressure environment on the compression behavior of ZnTe.

2. Experiments

A single crystal of ZnTe with a purity >99.99% (p-type) was powdered and loaded in a gasketed diamond-anvil cell [12]. The gasket made of a stainless steel was 100 μm thick and had a 120-μm-diameter hole. Two series of pressurization were carried out. In one series, a mixture of methanol, ethanol, and water in a ratio 16:3:1 in volume was used as a pressure-transmitting medium. Another series of pressurization was done without using the medium. The pressure was monitored by the ruby fluorescence line [13] with an accuracy of 0.2 GPa.

X-ray diffraction measurements were undertaken at BL-18C of the Photon Factory, Institute for Materials Structure Science,

---

* Corresponding address: University of Marketing and Distribution Sciences, Nishi-ku, Kobe 651-2188, Japan. Tel.: +81 75 751 7647; fax: +81 0 78 794 6149.

E-mail address: Akifumi_Onodera@red.umds.ac.jp (A. Onodera).

[1] Present address: University of Marketing and Distribution Sciences, Nishi-ku, Kobe 651-2188, Japan.
[2] Present address: Laboratory for Materials Structure Science, High Energy Accelerator Research Organization, Tsukuba, Ibaraki 305-0801, Japan.
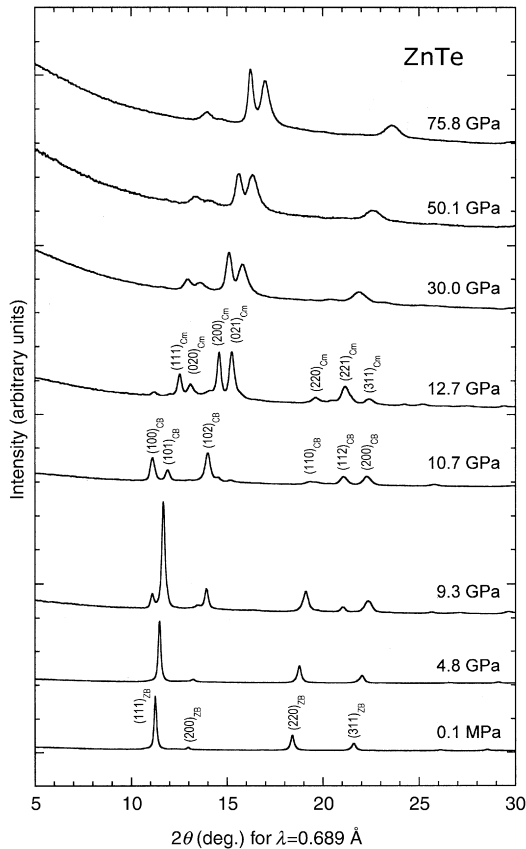
Fig. 1. X-ray diffraction patterns of ZnTe recorded at high pressure under compression using the pressure-transmitting medium. The suffices ZB, CB, and Cm attached to the indices stand for the zincblende-type, cinnabar-type, and *Cmcm*-type structures, respectively.

High Energy Accelerator Research Organization, Tsukuba. An incident beam with a wavelength of 0.689 Å was collimated to a size of 40 μm in diameter. Diffraction patterns were recorded on an imaging plate detector [14] with an exposure time of 25 min, typically.

3. Results and discussion

Fig. 1 shows the representative X-ray diffraction patterns of ZnTe pressurized with the pressure-transmitting medium. The patterns recorded at 0 and 4.8 GPa are from the zincblende-type phase (ZnTe-I). At 9.3 GPa, some lines from the cinnabar-type phase (ZnTe-II) appear in coexistence with the zincblende-type phase. The cinnabar-type phase becomes dominant at 10.7 GPa with a very slight amount of the *Cmcm*-type phase (ZnTe-III). The *Cmcm*-type phase prevails in the pattern recorded at 12.7 GPa and persists to the highest pressure studied, showing that this structure is stable to at least 76 GPa.

The same sequence in the phase transitions was observed when the ZnTe sample was pressurized without the medium. It turns out, in detail, that the two modes of pressurization give rise to a significant difference in the diffraction patterns. In Fig. 2(a) and (b), normalized d spacings (d_P/d_0) of six lines and normalized line width ($\Delta d/d$) of three lines from the zincblende-type phase (ZnTe-I) are respectively plotted against pressure. These parameters can describe uniaxial stress
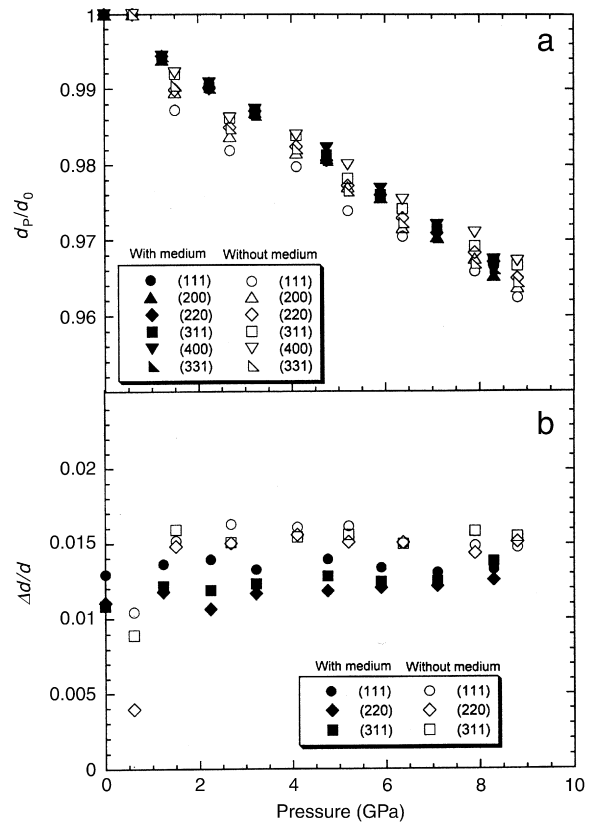

Fig. 2. (a) Normalized d spacings, d_P/d_0, of six lines from ZnTe-I (the zincblende-type phase); (b) normalized line width, $\Delta d/d$, of three lines from ZnTe-I.

and pressure gradient present in the sample under compression [15–17]. In brief, the presence of uniaxial stress causes both upward departure of d spacings and increase of $\Delta d/d$ with respect to hydrostatic condition, whereas a development of pressure gradient induces an increase of $\Delta d/d$ only [16]. In Fig. 2(a), the pressure dependence of d spacings with the pressure-transmitting medium is almost linear owing to the hydrostaticity achieved to 9 GPa by this medium [17]. Without the medium, the d spacings at pressures lower than 4 GPa are considerably smaller and approach at higher pressures to those with the medium. Fig. 2(b) shows that each $\Delta d/d$ with the medium remains almost unchanged upon the application of pressure. Without the medium, an abrupt increase in $\Delta d/d$ occurs at 1.5 GPa. At higher pressures, $\Delta d/d$ is kept constant and is clearly larger than that in the case where the pressure medium is employed.

Based on the hydrostaticity achieved with the present pressure-transmitting medium to at least 9 GPa [17], a combination of Fig. 2(a) and (b) leads to know the nature of pressure in ZnTe-I when the medium is not employed. The jump in $\Delta d/d$, Fig. 2(b), suggests a development of pressure gradient over the ZnTe sample. This is verified by a separate ruby fluorescence experiment which showed a gradient of ~0.8 GPa over the sample at 5 GPa. It should be noted that the profile of gradient changed with increasing pressure. Also, the ruby moved towards the periphery of sample space as the pressure was increased. Under such situations, the pressure
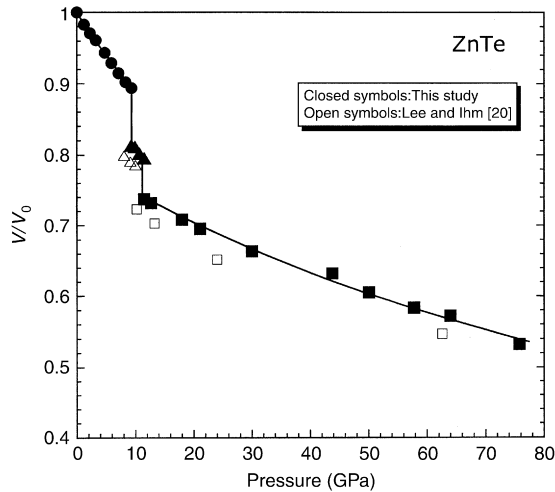
Fig. 3. Relative volume of ZnTe as a function of pressure (circle for ZnTe-I, triangle for ZnTe-II and square for ZnTe-III). The smoothed curves are the fits of the Birch–Murnaghan equation to the data. The fitting parameters are given in Table 2.

Table 1
Parameters for the phase transitions of ZnTe

ZnTe-I → ZnTe-II		ZnTe-II → ZnTe-III		Reference
P_t (GPa)	$\Delta V/V$ (%)	P_t (GPa)	$\Delta V/V$ (%)	
Experiment				
9.3(2)	9.0	10.7(2)	7.3	Present study
9.6	∼9	12.0		[6]
10.0(5)	8.8	12.0(5)		[7]
8.9		11.5	5.7(2)	[11]
9.5(5)	∼13	12.0(5)	∼13	[18]
9	12.0	13.0		[19]
Calculation				
8.06	10.1	10.24	7.7	[20]
5.9	1.1	11.0	8.4	[21]

at the X-rayed area could be eventually different from the pressure probed by the ruby. For instance, the departure of d spacings below 4 GPa, Fig. 2(a), can arise when the pressure at the X-rayed area is higher than that measured by the ruby fluorescence. Limited to ZnTe-I without the medium, uniaxial stress is absent in the sample as judged from the absence of upward departure in d spacings from the hydrostatic condition.

The considerations described above unequivocally show that the present pressure-transmitting medium provides the sample with hydrostatic condition at least in phase I (ZnTe-I). Any further discussion on the nature of pressure after the medium loses the hydrostaticity will not be dealt with. The following results are primarily limited to the experiment with pressure-transmitting medium.

Fig. 3 shows the pressure dependence of the relative volume of ZnTe. The ZnTe-I → ZnTe-II and ZnTe-II → ZnTe-III phase transitions are both accompanied by a large discontinuity in the volume. Table 1 shows the pressures and accompanying volume changes for the phase transitions, together with other investigations [6,7,11,18–21]. In Fig. 3, the calculation of Lee and Ihm [20] for ZnTe-II and ZnTe-III is smaller than our experimental data by about 3% and 5%, respectively. These authors, using *ab initio* pseudopotential, succeeded in deriving the structural sequence of pressure-induced phase transitions of ZnTe [20].

The bulk modulus B_0 and its pressure derivative B_0' of each phase of ZnTe were derived by a least squares fitting of the data shown in Fig. 3 with the Birch–Murnaghan equation [22]:

$$P = (3/2)B_0[(V/V_0)^{-7/3} - (V/V_0)^{-5/3}]\{1 + (3/4)(B_0' - 4)$$
$$\times [(V/V_0)^{-2/3} - 1]\} \tag{1}$$

where V and V_0 denote the volumes at pressure P and ambient pressure, respectively. Values of B_0 and B_0' derived without any constraint are shown in Table 2, along with other experiments [6,18,23] and calculations [20,21,24].

For the high-pressure phases of ZnTe, this is the first time to show the equation-of-state parameters. The bulk modulus of ZnTe-I obtained from the present study is the highest among the experiments. Other experiments give B_0 around 50 GPa, which is close to the present experiment without the medium, $B_0 = 57.4(6.2)$ GPa. The rough agreement may be interpreted by the presence of pressure gradient developed in the solid pressure-transmitting media employed in Refs. [6,23]. An exception to this argument is the study of San-Miguel et al. [18] since these authors used a liquid pressure-transmitting medium and, nevertheless, obtained B_0 values close to those from the solid pressure-transmitting media. Actually the liquid used in Ref. [18] was a silicone oil, and, the fact may be a point in any means. However, the current controversy on the hydrostatic limit of this material (for example it is reported to be higher than 15 GPa in Ref. [25] against a limit of ∼0.9 GPa in Ref. [26]) does not allow us to discuss in further detail.

In Table 2, most of the calculated values for the bulk modulus of ZnTe-I are in a range between 50 and 60 GPa. A pseudopotential calculation where d electrons are considered as a part of the core states [20] has yielded a higher value (70.5 GPa), which is eventually close to the present experiment.

It is of interest to see how the axial ratios of the cinnabar-type phase (ZnTe-II) and the *Cmcm*-type phase (ZnTe-III) change with pressure. The present experimental results are shown in Figs. 4 and 5, respectively. In Fig. 4, the c/a ratio of the cinnabar-type phase exhibits a slight decrease with increasing pressure, in agreement with the experiment of Nelmes et al. [10,11]. Thus the experimental data are against the calculation of Côté et al. [21] who show the c/a ratio to increase with pressure (although in Fig. 4 we show only one point that lies within the pressure range of interest). Fig. 5 shows that both the b/a and c/a ratios of the *Cmcm*-type phase remain constant over the pressure range studied. This fact suggests that the *Cmcm*-type lattice of ZnTe-III shrinks quite uniformly with pressure, irrespective of the pressure environment. The experimental data of Nelmes et al. [11] as well as the calculation of Lee and Ihm [20] fall into the group of the present data.

Table 2
Equation-of-state parameters for the three phases of ZnTe

ZnTe-I		ZnTe-II		ZnTe-III		Reference
B_0 (GPa)	B_0'	B_0 (GPa)	B_0'	B_0 (GPa)	B_0'	
Experiment						
76.4(1.7)	3.0(2)	91.3(7.0)	0.8(1.0)	134(5)	2.4(1)	Present study
51(3)	3.6(0.8)					[6]
50.5	5					[18]
56	5					[18]
48.8	3.7					[23]
Calculation						
52.9						[20]
70.5						[20]
88.0						[20]
54.7						[21]
51.2						[24]

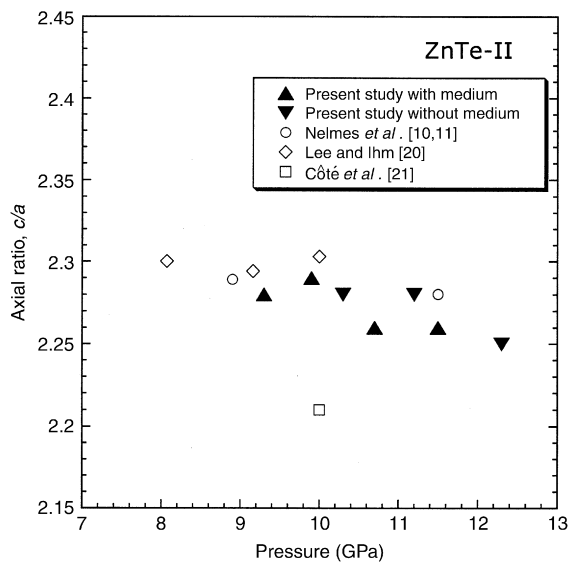Fig. 4. Pressure dependence of the axial ratio in the cinnabar-type phase of ZnTe (ZnTe-II).

Fig. 5. Pressure dependence of the axial ratios in the *Cmcm*-type phase of ZnTe (ZnTe-III).

4. Conclusions

The pressurization using a mixture of methanol, ethanol and water as the pressure-transmitting medium has yielded a bulk modulus of the zincblende-type phase of ZnTe (ZnTe-I) in fair agreement with one [20] of the *ab initio* calculations. The equation of states of the cinnabar-type and *Cmcm*-type phases, being the first experimental report, are both greater than an *ab initio* calculation [18] by 3%–5%.

References

[1] G.A. Samara, H.G. Drickamer, J. Phys. Chem. Solids 23 (1962) 457.
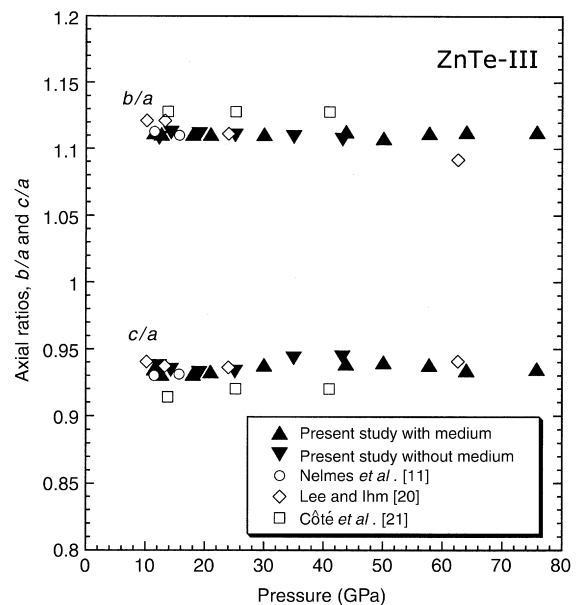[2] A. Ohtani, A. Onodera, N. Kawai, Rev. Sci. Instrum. 50 (1979) 308.
[3] A. Ohtani, M. Motobayashi, A. Onodera, Phys. Lett. 75A (1980) 435.
[4] S. Endo, A. Yoneda, M. Ichikawa, S. Tanaka, S. Kawabe, J. Phys. Soc. Jpn. 51 (1982) 138.
[5] A. Onodera, A. Ohtani, M. Motobayashi, O. Shimomura, H. Kawamura, Solid State Physics under Pressure: Recent Advances with Anvil Devices, KTK Sci. Publ., Tokyo, 1985, p. 141.
[6] K. Kusaba, L. Galoisy, Y. Wang, M.T. Vaughan, D.J. Weidner, PAGEOPH 141 (1993) 643.
[7] S.B. Qadri, E.F. Skelton, A.W. Webb, J.Z. Hu, in: S.C. Shmidt, J.W. Shaner, G.A. Samara, M. Ross (Eds.), High Pressure Science and Technology-1993, Part I, AIP Press, New York, 1994, p. 319.
[8] K. Kusaba, D.J. Weidner, in: S.C. Shmidt, J.W. Shaner, G.A. Samara, M. Ross (Eds.), High Pressure Science and Technology-1993, Part I, AIP Press, New York, 1994, p. 553.
[9] M.I. McMahon, R.J. Nelmes, N.G. Wright, D.R. Allan, in: S.C. Shmidt, J.W. Shaner, G.A. Samara, M. Ross (Eds.), High Pressure Science and Technology-1993, Part I, AIP Press, New York, 1994, p. 633.
[10] R.J. Nelmes, M.I. MaMahon, N.G. Wright, D.R. Allan, J. Phys. Chem. Solids 56 (1995) 545.
[11] R.J. Nelmes, M.I. MaMahon, N.G. Wright, D.R. Allan, Phys. Rev. Lett. 73 (1994) 1805.

[12] K. Takemura, O. Shimomura, K. Tsuji, S. Minomura, High Temp. High Press. 11 (1974) 311.

[13] H.K. Mao, P.M. Bell, J.W. Shaner, D.J. Steinberg, J. Appl. Phys. 49 (1978) 3276.

[14] O. Shimomura, K. Takemura, H. Fujihisa, Y. Fujii, Y. Ohishi, T. Kikegawa, Y. Amemiya, T. Matsushita, Rev. Sci. Instrum. 63 (1992) 967.

[15] J.W. Otto, J.K. Vassiliou, G. Frommeyer, Phys. Rev. B57 (1998) 3253.

[16] K. Takemura, J. Appl. Phys. 89 (2001) 662.

[17] K. Takemura, P.Ch. Sahu, Y. Kuni, Y. Toma, Rev. Sci. Instrum. 72 (2001) 3873.

[18] A. San-Miguel, A. Polian, M. Gautier, J.P. Itié, Phys. Rev. B48 (1993) 8683.

[19] O. Shimomura, W. Utsumi, T. Urakawa, T. Kikegawa, K. Kusaba, A. Onodera, The Review of High Pressure Science and Technology (special issue) 6 (1997) 207.

[20] G.-D. Lee, J. Ihm, Phys. Rev. B53 (1996) R7622.

[21] M. Côté, O. Zakharov, A. Rubio, M. Cohen, Phys. Rev. B55 (1997) 13025.

[22] F. Birch, J. Geophys. Res. 83 (1978) 1257.

[23] O. Shimomura, W. Utsumi, S. Urakawa, M. Yamakata, T. Kikegawa, A. Onodera, Proc. 33rd High Pressure Conf. Japan, 1992 p. 464.

[24] M.L. Cohen, in: M.H. Manghnani, W.J. Nellis, M.F. Nicol (Eds.), Proceeding of AIRAPT17 (Science and Technology of High Pressure), University Press, Hyderabad, India, 2000, p. 900.

[25] D.D. Ragan, D.R. Clarke, D. Schiferl, Rev. Sci. Instrum. 67 (1996) 494.

[26] R.J. Angel, M. Bujak, J. Zhao, G.D. Gatta, S.D. Jacobson, J. Appl. Crystallogr. 40 (2007) 26.